Brain Plasticity 6 (2020) 123–136
DOI 10.3233/BPL-200110
IOS Press

Research Report

Effects of Ethanol on Synaptic Plasticity and NMDA Currents in the Juvenile Rat Dentate Gyrus

Scott D. Sawchuk[a], Hannah M.O. Reid[a], Katie J. Neale[a], James Shin[a] and Brian R. Christie[a,b,c,*]
[a]*Division of Medical Sciences, University of Victoria, Victoria, BC, Canada*
[b]*Department of Psychology, University of British Columbia, Vancouver, BC, Canada*
[c]*Island Medical Program and Department of Cellular and Physiological Sciences, University of British Columbia, Victoria, BC, Canada*

Abstract.
Background and Objectives: We examined how acute ethanol (EtOH) exposure affects long term depression (LTD) in the dentate gyrus (DG) of the hippocampus in juvenile rats. EtOH is thought to directly modulate n-methyl-D-aspartate receptor (NMDAr) currents, which are believed important for LTD induction. LTD in turn is believed to play an important developmental role in the hippocampus by facilitating synaptic pruning.
Methods: Hippocampal slices (350 μm) were obtained at post-natal day (PND) 14, 21, or 28. Field EPSPs (excitatory post-synaptic potential) or whole-cell EPSCs (excitatory post-synaptic conductance) were recorded from the DG (dentate gyrus) in response to medial perforant path activation. Low-frequency stimulation (LFS; 900 pulses; 120 s pulse) was used to induce LTD.
Results: Whole-cell recordings indicated that EtOH exposure at 50mM did not significantly impact ensemble NMDAr EPSCs in slices obtained from animals in the PND14 or 21 groups, but it reliably produced a modest inhibition in the PND28 group. Increasing the concentration to 100 mM resulted in a modest inhibition of NMDAr EPSCs in all three groups. LTD induction and maintenance was equivalent in magnitude in all three age groups in control conditions, however, and surprisingly, NMDA antagonist AP5 only reliably blocked LTD in the PND21 and 28 age groups. The application of 50 mM EtOH attenuated LTD in all three age groups, however increasing the concentration to 100 mM did not reliably inhibit LTD.
Conclusions: These results indicate that the effect of EtOH on NMDAr-EPSCs recorded from DGCs is both age and concentration dependent in juveniles. Low concentrations of EtOH can attenuate, but did not block LTD in the DG. The effects of EtOH on LTD do not align well with it's effects on NNMDA receptors.

Keywords: Ethanol, dentate gyrus, hippocampus, long-term depression, NMDA, n-methyl-D-aspartate

INTRODUCTION

Alcohols are organic molecules assembled from Carbon, oxygen and hydrogen atoms, and when two carbons are present, the alcohol is known as ethanol (EtOH), or ethyl alcohol. EtOH is the form of alcohol that contained in most alcoholic beverages, and is one of the most widely used and abused drugs in the modern world [1]. Excessive consumption of EtOH has been shown to significantly impair learning and memory processes [2, 3]. The neurological effects of EtOH depend upon the amount consumed, and can

*Correspondence to: Brian R. Christie, Division of Medical Sciences, University of Victoria, 3800 Finnerty Rd, Victoria, BC V8P 5C2, Canada. E-mail: brain64@uvic.ca.

ISSN 2213-6304/20/$35.00 © 2020 – IOS Press and the authors. All rights reserved
This article is published online with Open Access and distributed under the terms of the Creative Commons Attribution Non-Commercial License (CC BY-NC 4.0).

range from being anxiolytic at lower doses, to producing partial to complete memory loss with higher doses [4]. While these behavioral effects are well-recognized, the acute effects of EtOH on neuronal function remain poorly understood.

EtOH is known to acutely modulate both inhibitory and excitatory receptors. At inhibitory receptors, it is thought that EtOH binds to a site that is separate from the gamma aminobutyric acid (GABA) binding site, where it can act as a positive allosteric modulator to enhance the inhibitory effects of GABA [5]. There is also support for GABA receptors mediating the anxiolytic and mood-enhancing effects of alcohol [5], however these effects seem to be particularly relevant at low (<30 mM) EtOH concentrations. At concentrations of 50 mM or greater, EtOH is thought to exert effects on learning and memory processes by directly affecting the function of NMDArs [6–12].

Although it is widely accepted that EtOH acutely inhibits NMDArs, several studies suggest that the sensitivity of neurons to EtOH varies across CNS regions, and that its efficacy also varies as a function of developmental age [13, 14]. NMDArs are calcium-permeable heteromeric ion channels, composed of two obligatory GluN1 subunits and two additional GluN2 (A, B, C, D) or GluN3 (A, B) subunits [15]. Each receptor requires the binding of both glycine (to GluN1) and glutamate (to GluN2) for activation [16], and the GluN2 subunits play a critical role in determining many of the electrophysiological properties of the receptor. Studies in oocytes indicate that NMDArs do not respond uniformly to EtOH, and that receptors containing GluN2A or GluN2B subunits are more sensitive to EtOH than those containing GluN2C/D [17, 18]. EtOH is a partial NMDAr antagonist that inhibits NMDAr-EPSCs over a range of concentrations (1 : 100 mM [19–21]), however the inhibition generally remains incomplete even under extreme experimental circumstances (100–500 mM; [19, 22]). There are at least four different residue sites that EtOH can interact with on NMDArs, with sites on the GluN1 and GluN2 subunits regulating both receptor kinetics and EtOH sensitivity. The appositional location of these residues may play a role in the ability of EtOH to regulate receptor activity [23–25].

Synaptic plasticity is the main biological candidate for a learning and memory mechanism, and NMDArs are thought to play a role in both long-term potentiation (LTP) and long-term depression (LTD) of synaptic efficacy in the hippocampus [26, 27]. EtOH has been repeatedly shown to inhibit LTP induction *in vitro* [26, 27], however it remains controversial as to how LTD is impacted. To date, *in vitro* studies have had conflicting results with one group showing enhancement of LTD with EtOH [8], while a second group has shown that EtOH can inhibit of LTD [9]. Because NMDAr subunit composition can change during development, we used whole-cell recordings and field electrophysiology to examine the effects of moderate (50 mM) and high (100 mM) concentrations of EtOH on both NMDAr currents and LTD in the DG of hippocampal slices.

MATERIALS AND METHODS

Subjects

All animal procedures were performed in accordance with Canada Council on Animal Care guidelines and were approved by the University of Victoria animal care committee. Male and Female Sprague Dawley rats were obtained from Charles River (Ontario, Canada) and bred in house. The day of birth was considered PND0 and pups were weaned at post-natal day (PND) 21. After weaning, animals were separated by sex and group housed (2–3 animals) in standard rat cages with enrichment and ad libitum access to water and standard rat chow. Rats were kept on a 12-hour light/dark cycle in a room with a constant ambient temperature ($21 \pm 1°C$) and humidity ($50\% \pm 7\%$) and were randomly assigned for experimentation at one of three time points: PND14 (PND 13–15), PND21 (PND 20–26), and PND28 (PND 27–30). The average weights of rats in grams for each group was: PND14 : 31.83 ± 0.67; PND 21 : 56.69 ± 1.08; and PND28 : 98.61 ± 1.49.

Tissue preparation

Fresh artificial cerebral spinal fluid (aCSF) was prepared daily for all experiments. For field recordings, the aCSF was composed of (in mM): 125 NaCl, 2.5 KCl, 1.25 NaH2PO4, 25 NaHCO3, 2 CaCl2, and 1.3 MgCl2 and was bubbled continuously with carbogen (95% O2 / 5% CO2; 295–305 mOsm; pH 7.2). For patch-clamp recordings, we used a high sucrose cutting solution containing (in mM): 200 Sucrose, 2.5 KCl, 1.25 NaH2PO4, 25 NaHCO3, 0.5 CaCl2, 7 MgCl2, 10 dextrose, 1 Ascorbic Acid, and 3 Na-pyruvate. To acquire slices, rats were deeply anaesthetized with isoflurane, decapitated, and the brain was rapidly excised in chilled aCSF. The brain was then placed on its ventral surface on a chilled petri dish, and blocked by removing the cerebellum

and the prefrontal cortex. The two hemispheres were separated by making an incision along the midline with a scalpel. Each hemisphere was then placed on its midsagittal side, and a sliver of dorsal cortex was excised with the blade angled inwards at ∼30 degrees relative to the cutting surface. This created a flat surface of dorsal cortex that could be glued to the vibratome stage, and help create slices where the dendritic axis of granule cells remain parallel to the cutting plane. For all experiments, 350 μm–400 μm transverse slices were cut in chilled aCSF using a vibratome (1500 Ted Pella, Inc., CA, USA). Each slice was immediately transferred to normal aCSF and incubated at 32°C for 30 min. Slices were then left for an additional 30 min at room temperature before being transferred individually to a recording chamber. For recordings, all slices were perfused with oxygenated aCSF (2–3 mL/min) at 29.9 ± 1°C.

Extracellular field electrophysiology

All fEPSPs were recorded from the suprapyramidal blade of the DG using regular ACSF as described previously [28]. Briefly, slices were visualized using an upright Olympus BX51WI microscope and evoked responses were amplified with either an Axopatch 200B or Multiclamp 700B; filtered at 10 kHz with a low-pass Bessel filter and digitized at a rate of 100 kHz (10 μs) (Digidata1440 or 1550b). A Sutter P-1000 micropipette puller was used to create recording electrode pipettes (1 MΩ) that were then back-filled with normal aCSF. The recording and stimulating electrodes (concentric bipolar pt/ir; FHC, Bowdoin, ME, USA) were both placed into the middle third of the molecular layer, approximately 200 μm apart and equidistant to the outer edge of the granule cell layer (GCL), to stimulate the MPP (medial perforant path) input. Small (1–2 μm) adjustments in the relative depth of the electrodes in the tissue were then made to optimize the size of the evoked fEPSP. All data acquisition was performed using a pulse width of 120 μs, and fEPSP response was adjusted to 60–80% of the maximum fEPSP by adjusting the current amplitude.

To determine stimulus – response relationships for each slice, an Input/Output (IO) curve was generated at the beginning of each experiment by delivering a series of square current pulses (30 μs to 300 μs) at 0.1 Hz. Next, a series of paired pulses (50 ms interpulse interval) were delivered at a rate of 0.067 Hz to ensure that the electrode positions did not result in the significant facilitation normally observed with lateral perforant path electrode positions [28].

Prior to the application of any conditioning stimuli or pharmacological agents, a stable baseline was acquired at a rate of 0.067 Hz for a minimum of 20 minutes. Low-frequency stimulation (LFS) was induced by administering a train of 900 pulses at 1 Hz (120 μs pulse width) as baseline. Unless otherwise stated, drug application was restricted to a period of 5 minutes prior to LFS, and remained in the perfusate for the duration of the conditioning stimulus. The perfusate then was switched back to regular aCSF immediately following the LFS period. The degree of change in the fEPSP slope was used to evaluate changes in post-tetanic potentiation (PTP; 0–5 min post-LFS) or LTP (55–60 min post-LFS). The slope of the initial negative phase of the fEPSP was used to isolate the monosynaptic response from the fiber volley, while also avoiding contamination of the signal by disynaptic components [28]. The fEPSP was analyzed using custom written data analysis software (www.github.com/NRSC/projDGDev) using the R programming language. The slope was calculated by fitting a linear model between 20% and 60% of the falling phase of the EPSP for each individual sweep. Slices were omitted if the fitting a linear regression model to the 15 minutes of baseline preceding the conditioning stimulus resulted in a slope coefficient with an absolute value greater than 0.75.

Whole-cell patch clamp electrophysiology

Whole-cell recordings were made in an oxygenated aCSF containing (in mM): 119 NaCl, 3 KCl; 1.25 NaHPO4; 25 NaHCO3; 1.3 CaCl2; 1 MgCl2; 10 dextrose; 1 Ascorbic Acid; and 3 Na-pyruvate (295–305 mOsm; pH of 7.4). Pipette tips (4–6 MΩ) were pulled with a Sutter P-1000 micropipette puller and filled with intracellular pipette solution containing (in mM): 123 CsMeSO4; 7 CsCl; 5 EGTA; 10 HEPES; 1 CaCl2; 5 Phosphocreatine Tris; 3 MgATP, 0.2 GTP Tris, 5 QX-314 Bromide (285 mOsm, pH 7.3). For whole-cell recordings only, picrotoxin (100 μM in DMSO) was added to the modified aCSF to block fast inhibitory GABAA channels. EPSCs were recorded from DGCs located in the suprapyramidal blade of the DGL. Slices were visualized under an upright fixed stage Olympus BX51W1 microscope and perfused with modified aCSF, oxygenated with 95% O2/ 5% CO2 at 2–3 mL/min at 32°C ± 1°C. Individual DGCs were visually selected using oblique illumination, and cell access was obtained in voltage-clamp mode after acquiring seals >1 G. The liquid junction potential was corrected for

and DGCs were voltage-clamped at –70 mV. To evaluate NMDAr responses, cells were briefly stepped to +40 mV. EPSC responses were adjusted to 40–60% of their maximum AMPA response after stimulation of the MPP (0.0334 Hz). NMDAr-EPSCs were analyzed 50 ms after the current onset. Passive electrical properties of the cell were monitored with a 5 mV hyperpolarizing test pulse, and series resistance (Rs) was not compensated for. Cells with Rs > 30 MΩ, or that showed changes to the Rs >than 20% were omitted.

Drugs

All drugs were purchased from Sigma-Aldrich (St. Louis, MO) or Tocris Biosciences (Burlington, ON). EtOH (95%) was acquired from the university stores facility and added to the aCSF immediately prior to wash-in. Stock solutions of DL-AP5 (10 mM) were made in distilled water and stored at –20°C.

Statistics

Statistics were computed using the R-Project for statistical computing [29]. Packages utilized for the analysis and presentation of data include ggplot2 [30], gginnards [31], data.table [32], kableExtra [33], knitr [34], lme4 [35], PNG [36], rMarkdown [37], roxygen2 [38], tidyverse [39], usethis [40] and yaml [41]. All data are presented as mean ± standard error of the mean (SEM). Statistical differences were determined by two-tailed student *t*-test or one-way analysis of variance (ANOVA) followed by the appropriate *post-hoc* test. The level for statistical significance was $p < 0.05$.

RESULTS

Developmental influences the effects of EtOH on NMDAr EPSCs

To determine the effects of EtOH on NMDAr-EPSCs in the developing DG, whole-cell patch clamp recordings were employed in conjunction with acute exposure to either 50 mM or 100 mM EtOH. When 50 mM EtOH was added to the aCSF, there was relatively little effect on NMDAr-EPSCs at PND14 (100.71 + 5.79) and at PND21 (104.73 + 3.87; Fig. 1). At PND28, the EPSC magnitude was slightly decreased (87.79 + 7.01). Increasing the EtOH concentration to 100 mM produced a general trend towards inhibition that was apparent in all three age groups, however an ANOVA revealed no significant effect of either 50 mM or 100 mM EtOH at any time point (PND14 : 89.11 + 5.74; PND21 : 89.25 + 8.44; PND28 : 89.11 + 5.74). As is illustrated in Fig. 2, the addition of EtOH (50 or 100 mM) to the bath perfusion did not significantly alter the stability of the evoked EPSCs.

LFS produces equivalent magnitudes of LTD across the juvenile period (PND12-30)

The application of LFS (900 × 1 Hz) at DG-MPP synapses induced a reliable decrease in the fEPSP slope in all three age groups ($p < 0.05$). The average change in the EPSP slope for each group was: PND14 (–15.08 + 1.76%, slices = 22, animals = 12), PND21 (–14.31 + 2.53%, slices = 24, animals = 13), and PND28 (–12.14 + 1.75%, slices = 35, animals = 15; Fig. 3). No significant differences were seen in the magnitude of LTD induced at each age group as determined by one way ANOVA ($F(2,78) = 0.594$, $p = 0.56$). One way ANOVA revealed no significant differences in the magnitude of LTD induced when subjects were grouped by sex ($F(1,79) = 0.001$, $p = 0.97$). A decrease in the slope of the fEPSP greater than 10% of baseline was observed in 86.36%, 58.33%, and 60% of slices at PNDs 14, 21 and 28 respectively, and a percentage of slices in each age group (PND14 : 4.55%, PND21 : 4.17%, and PND28 17.14%) showed a potentiation of the EPSP slope after LFS. Notably, LTD was induced without increasing the strength of the conditioning stimulus when the 900 pulses were applied, and no slices in any age group showed a potentiation of the EPSP slope greater than 10% following the application of these stimuli.

A number of slices from two of the age groups (PND 21: $n = 5$; PND 28: $n = 12$) were also obtained using a sucrose cutting solution that is often preferred for whole-cell recordings [42], however the amount of LTD induced in these slices did not differ significantly from that observed in those cut in normal aCSF (Sucrose: –13.37 + 2.3%, ACSF: –14.07 + 3.48%; pairwise *t*-test, $p = 0.48$; data not shown).

AP5 inhibits LTD in the DG at PND21 and PND28, but not at PND14

To determine the role of NMDArs in LFS-induced LTD in the DG over the juvenile developmental period, we examined the capacity of LFS

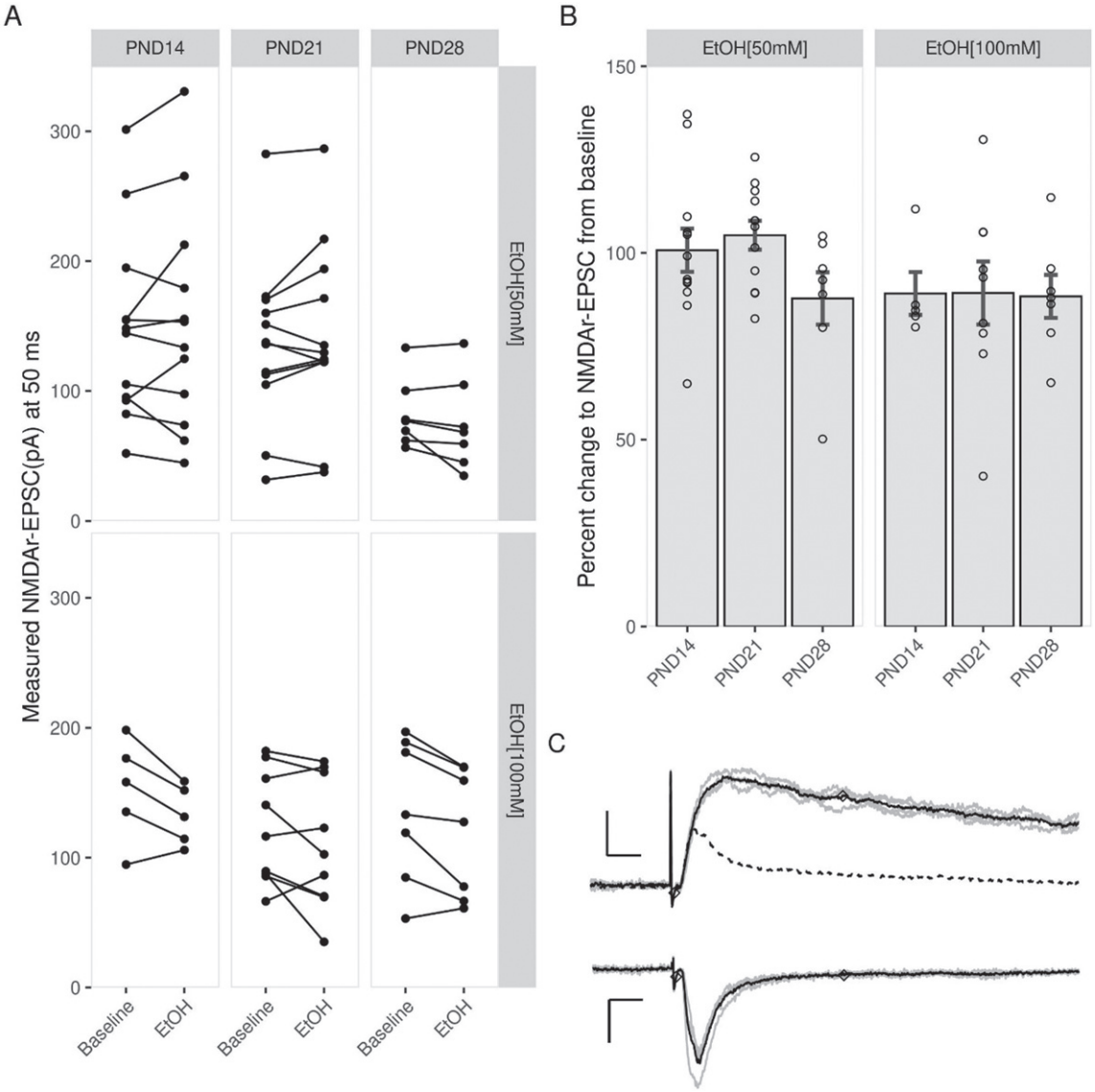

Fig. 1. Summary of the acute effects of EtOH on NMDArs. (A) Magnitude (in pA) of NMDAr-EPSCs measured 50 ms after the onset of an evoked response before (Baseline) and after EtOH exposure. (B) Percent change in NMDAr-EPSCs after EtOH wash in. 50 mM EtOH did not produce a consistent effect at PND14 and PND21, but reduced NMDAr-EPSC size in slices from animals at PND28. 100 mM EtOH reduced the magnitude of NMDAr-EPSCs in all juvenile age groups. (C) Representative traces recorded at either –70 mV (bottom) or +40 mV (top) showing how receptor kinetics were used to isolate the NMDAr response (top) from the AMPA response (bottom). Data points indicate mean ± SEM.

to induce LTD in the three age groups in the presence of AP5 (50 μM). Under these conditions, LFS induced LTD was still observed in slices at PND14 (–14.03 + 1.9%, slices = 9, animals = 7), however AP5 blocked LTD induction in both the PND21 (0.14 + 3.19%, slices = 15, animals = 7), and the PND28 (0.75 + 3.69%, slices = 10, animals = 5; Fig. 4) groups. A two-way ANOVA revealed a significant interaction of age and treatment ($F(2,109) = 3.37$, $p = 0.038$), and follow up *post-hoc* analysis revealed a significant effect of treatment with AP5 at PND21 and PND28 ($p = 0.00095$, $p = 0.0122$; *post-hoc* pairwise comparisons with Bonferroni correction). Significant differences were revealed when comparing the effects of AP5 at the early juvenile time period (PND14) with the later juvenile groups (PND21: $p = 0.024$, PND28: $p = 0.035$; *post-hoc* pairwise comparisons with Bonferroni correction). Thus,

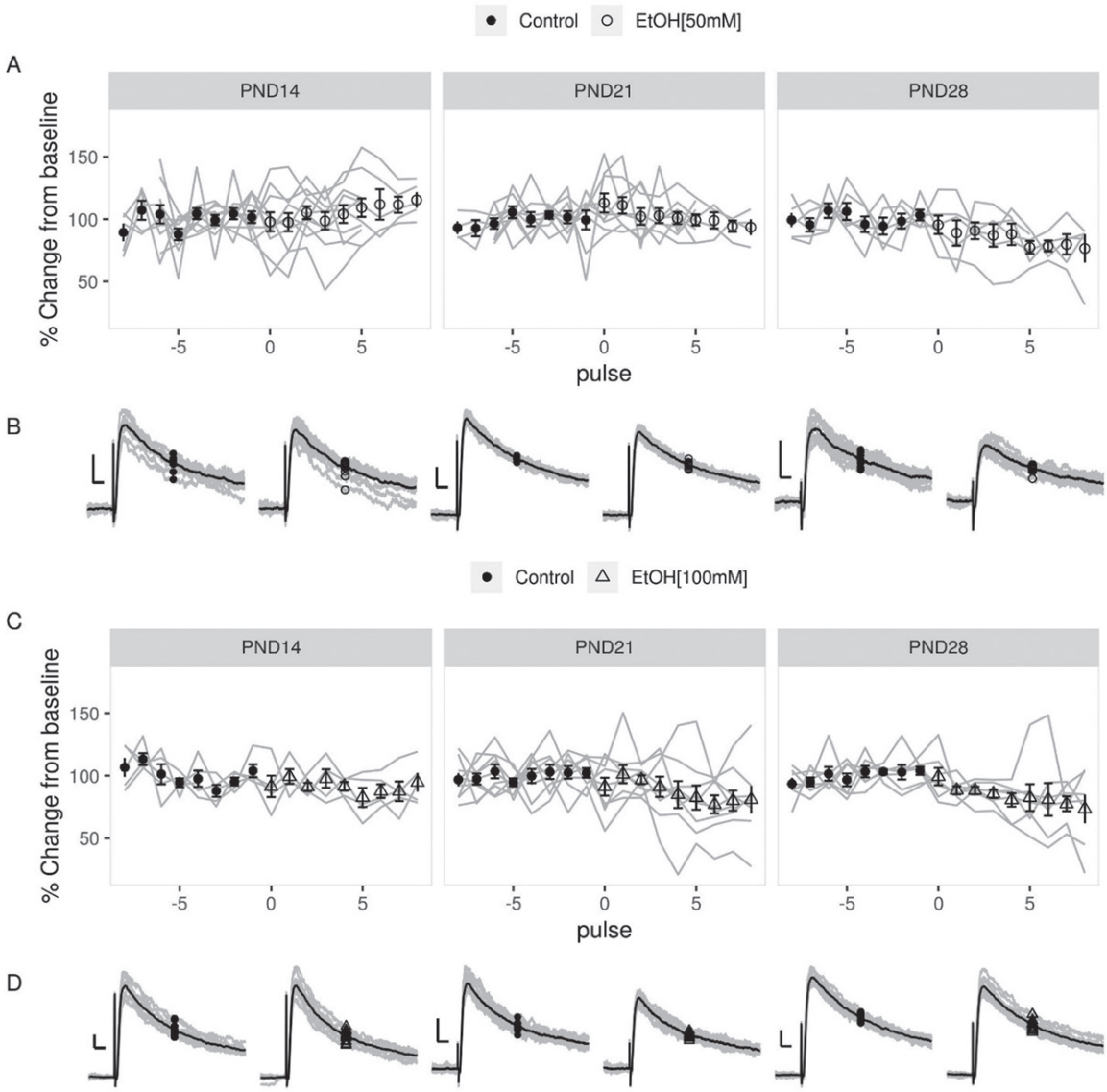

Fig. 2. No effect of EtOH on NMDAr-EPSCs amplitude throughout patch-clamp experiments. Scatterplots of percent change relative to baseline for EtOH [50 mM] (A) and EtOH [100 mM] (C) whole-cell experiments. Note that the inclusion of ethanol (A: 50 mM or C: 100 mM) in the perfusion did not significantly impact EPSC amplitude at any time point. Below (A) and (C) are representative NMDAr-EPSCs for each age group, showing EPSCs before (left) and after (right) exposure to EtOH. EPSCs were collected in regular aCSF (closed circles or triangles) or in the presence of EtOH. (50 mM: Open circles; 100 mM: open triangles). Markers along traces indicate the point 50 ms after the onset of the EPSC where the magnitude of the response was measured. Scale bars: 5 ms and 10 pA. Data points indicate mean ± SEM.

the role of NMDARs in LTD induction appears to increase with age.

Low, but not high, concentrations of EtOH attenuate LTD in the DG

The next experiments examined the capacity for acute EtOH application (50 or 100 mM) to modulate LFS induced LTD in the DG. Because the duration of EtOH exposure can potentially impact the induction of LTD (44), care was taken to expose slices from all age groups equivalently to EtOH (<5 minutes prior to LFS). Given the high volatility of EtOH, it was consistently added to the oxygenated aCSF immediately prior to bath application to ensure a greater uniformity across groups. In all three age groups, 50 mM EtOH attenuated the induction of LTD with the LFS (PND14: –7.47 + 3.45%; PND21:

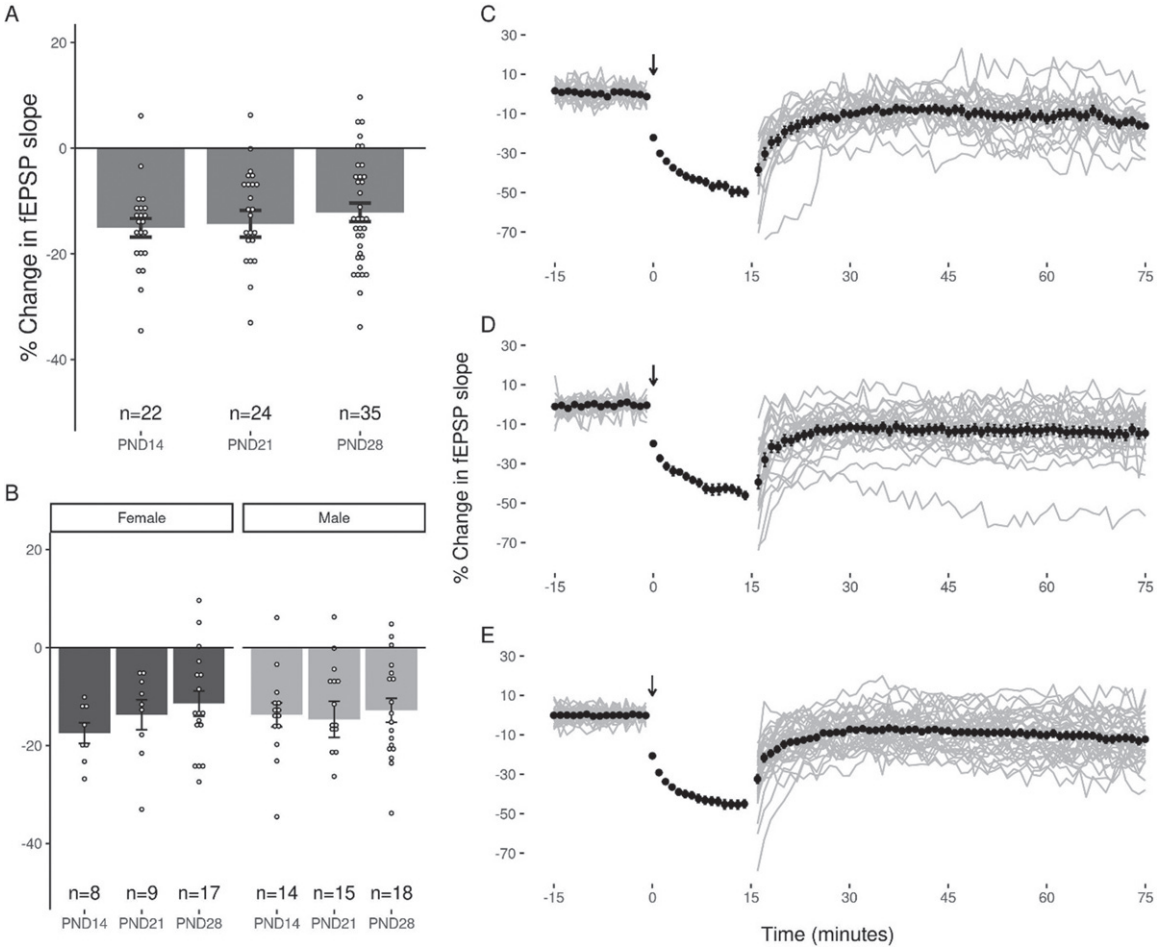

Fig. 3. Equivalent LTD of the DG fEPSP slope across the juvenile period. (A) LFS induced a decrease in the fEPSP that was greater than 10% in 87%, 59%, and 60% of slices at PND14, 21 and 28 respectively. This was not associated with a statistically significant difference in the magnitude of LTD induced between groups. (B) No significant effect of sex was observed in any juvenile age group. (C, D, E) Representative figures showing the induction and expression of LTD after LFS for PND14 (C), PND21 (D), and PND28 (E) age groups respectively. LTD was quantified by comparing the magnitude of the slopes for responses averaged over the 5 minutes directly preceding LFS to those averaged over the last 5 minutes of the 60-minute decay period. Data points indicate mean ± SEM.

–6.52 + 3.15%; PND28: –5.03 + 1.5%; Fig. 5). A two-way ANOVA revealed a significant main effect of treatment with 50 mM EtOH on the magnitude of LTD induced ($F(1,105) = 11.37$, $p = 0.0011$) compared to controls, and no significant effect of age ($F(2,105) = 0.769$, $p = 0.466$). Follow up *post-hoc* analyses indicated that LTD was significantly inhibited at PND14 ($p = 0.048$) and PND28 ($p = 0.043$), with a trend towards inhibition at PND21 ($p = 0.069$; *post-hoc* pairwise comparisons with Bonferroni correction). In contrast to the effects observed with 50 mM EtOH, the application of 100 mM EtOH did not significantly attenuate LTD induction (PND14: –16.65 + 3.31%; PND21: –10.94 + 3.31%; PND28: –7.55 + 4.03%; 2-way ANOVA: treatment $F(1,105) = 1.887$, $p = 0.172$; age $F(2,105) = 0.449$, $p = 0.639$; Fig. 6).

DISCUSSION

There are several important findings that arose from this data set. First, equivalent levels of LTD can be induced in the MPP input to the DG across the juvenile period (PND12-30). The LTD was reliably induced at the same stimulus strength used to evoke EPSPs in the pre- and post-conditioning baseline periods, indicating that an increase in stimulus strength is not required for reliable LTD induction in the DG. Although the magnitude of LTD was consistent across the juvenile period, as is shown in

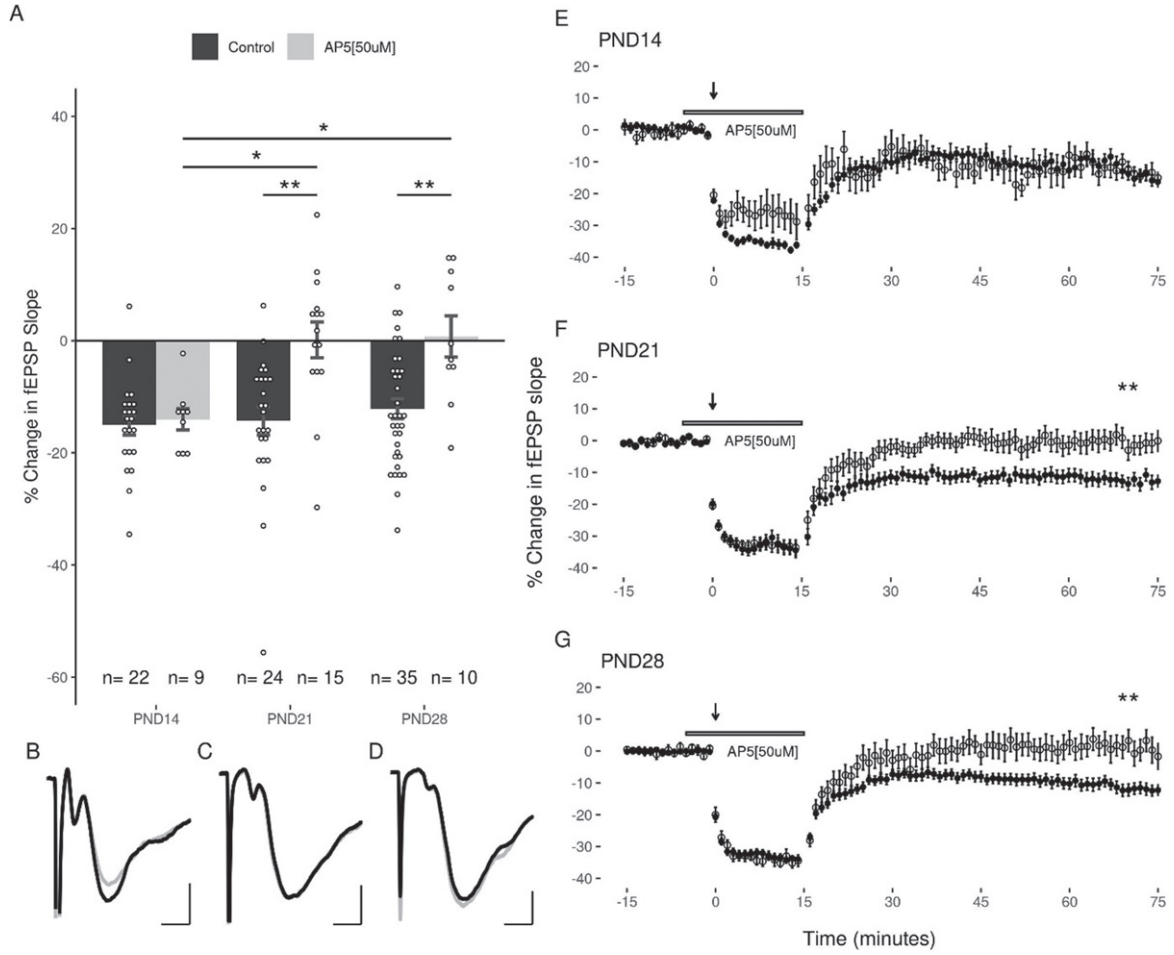

Fig. 4. NMDA antagonists significantly inhibit LTD in slices at PND21 and PND28 groups, but not at PND14. (A) Significant differences were observed between the effects of AP5 when comparing the early juvenile group (PND14) to the PND21 and PND28 groups ($p = 0.01$; n (M/F) = 5/4, 9/6, 5/5). (B, C, D) Representative traces of the fEPSP before conditioning (black), and after a 60-minute decay period (grey) for PND14, PND21, and PND28 age groups respectively. Scale bars: 0.5 mV and 2 ms. (E, F, G) Representative figures showing the induction and expression of LTD after LFS, and the effects of AP5 on recovery of the response for PND14, PND21, and PND28 age groups respectively. LTD was quantified by comparing the magnitude of the slopes for responses averaged over the 5 minutes directly preceding LFS to those averaged over the last 5 minutes of the 60-minute decay period. Data points indicate mean ± SEM. $^{*}p < 0.05$; $^{**}p < 0.01$.

Fig. 7, there were age-dependent differences in the capacity of NMDAr-antagonists and EtOH to modulate the magnitude of LTD. NMDAr antagonists did not block LTD induction in the youngest age group (PND14), although it did reliably block LTD in the two older juvenile age groups. Lower concentrations of EtOH (50 mM) significantly attenuated LTD in all three age groups, however the higher concentration (100 mM) was surprisingly ineffective in reducing LTD expression. The voltage-clamp data indicated that 50 mM EtOH had disparate effects on NMDAr currents in the three age groups, while 100 mM EtOH induced minor, but not significant, reductions in the magnitude of the recorded EPSCs. Taken together, these results indicate that the role of NMDA receptors in LTD evolves over the course of the juvenile period, and that EtOH only seems to act as a weak antagonist of NMDAr mediated EPSCs in the DG. Indeed, the acute effects of 50 mM EtOH on NMDAr mediated EPSCs at PND14 and PND21 are in contrast to what was expected based upon the literature [7, 20, 43–45]. While developmental time point and cell type likely play significant roles in discrepancies seen between this work and the literature, differences in methodology are also important factors to consider.

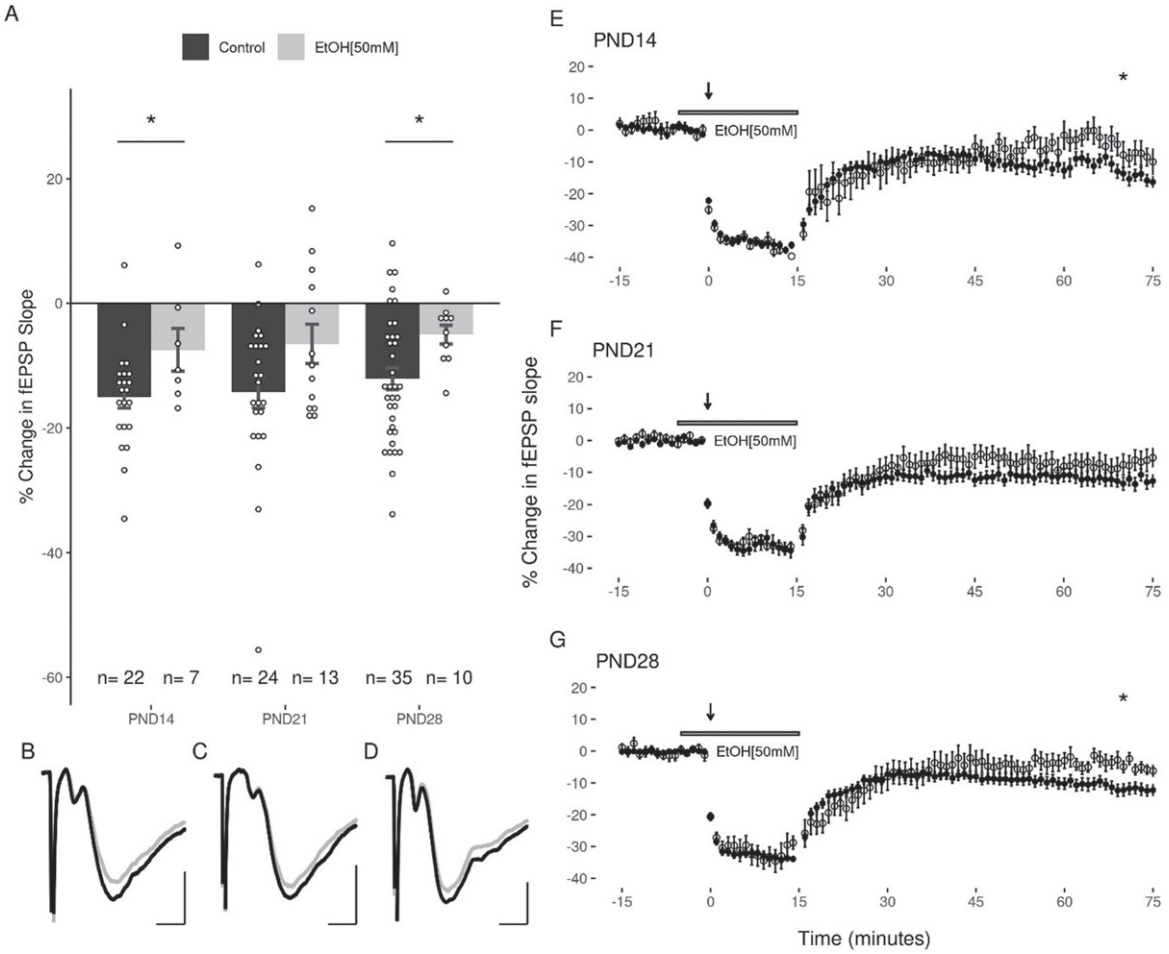

Fig. 5. LTD is significantly inhibited by 50 mM EtOH at PND14 and PND28, but not at PND21. (A) No significant differences were observed when comparing the effects of 50 mM EtOH between age groups (n(M/F) = 4/3, 6/7, 4/6). (B, C, D) Representative traces of the fEPSP before conditioning (black), and after a 60-minute decay period (grey) for PND14, PND21, and PND28 age groups respectively. Scale bars: 2 ms and 0.5 mV. (E, F, G) Representative figures showing the induction and expression of LTD after LFS in the presence of 50 mM EtOH for PND14, PND21, and PND28 age groups respectively. LTD was quantified by comparing the magnitude of the slopes for responses averaged over the 5 minutes directly preceding LFS to those averaged over the last 5 minutes of the 60-minute decay period. Data points indicate mean ± SEM. $^*p < 0.05$.

EtOH has been well characterized as a partial NMDAr antagonist [22, 46–49], but relatively little work has gone into looking at the acute effects of EtOH on NMDAr-mediated EPSCs in the DG [20, 43]. Prior studies have suggested that higher concentrations of EtOH can partially inhibit NMDAr currents in dentate granule cells. EtOH (75 mM) depressed the amplitude of evoked population action potentials, inhibited 5 Hz potentiation, and blocked 50–60% of the NMDAr-mediated EPSCs in 12–30 day old Sprague-Dawley rat slices *in vitro* [43]. Similarly, EtOH concentrations up to 80 mM have been shown to inhibit NMDAr EPSC's by up 50% in DG cells from both rat and monkey, while having no effect on basic membrane properties [20]. In our study we found evidence that EtOH can have both concentration and age-dependent effects in juvenile rats.

Understanding how EtOH impacts neuronal function in the DG is important, however this is also a complex issue in areas like the DG that show persistent neurogenic activity throughout adulthood. The sensitivity of individual receptors to EtOH depends upon the specific combination of GluN1 and GluN2 subunits present at synapses [10], and there are significant developmental changes to NMDAr subunit expression in DGCs as they mature [50–52]. Increases to the ratio of GluN2A:GluN2B subunits are often reported throughout neuron development

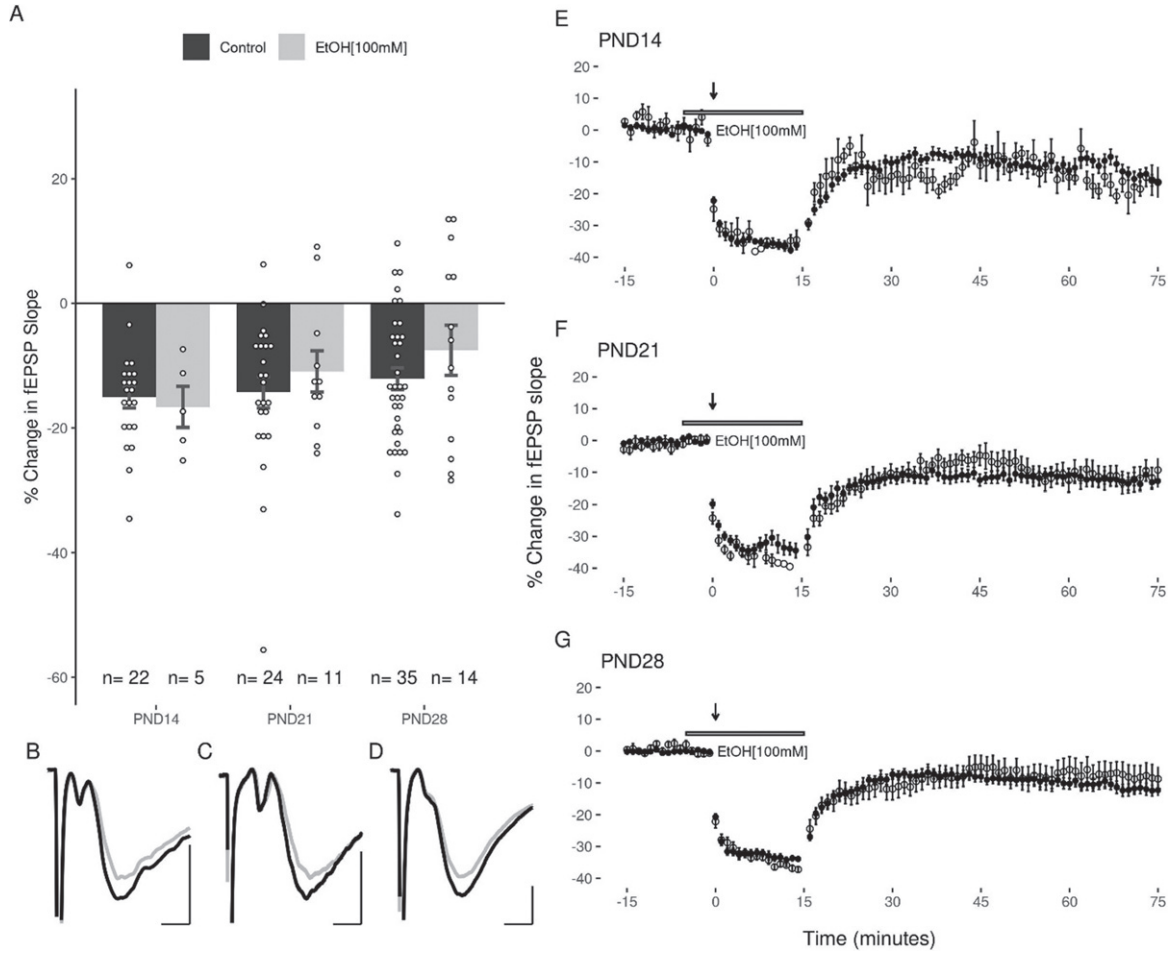

Fig. 6. LTD is not inhibited by 100 mM EtOH in the DG of juvenile animals. (A) LFS reliably induced LTD in all age groups (n (M/F) = 3/2, 3/8, 7/7). (B, C, D) Representative traces of the fEPSP before conditioning (black), and after a 60-minute decay period (grey) for PND14, PND21, and PND28 age groups respectively. Scale bars: 2 ms and 0.5 mV. (E, F, G) Representative figures showing the induction and expression of LTD after LFS in the presence of 100 mM EtOH for PND14, PND21, and PND28 age groups respectively. LTD was quantified by comparing the magnitude of the slopes for responses averaged over the 5 minutes directly preceding LFS to those averaged over the last 5 minutes of the 60-minute decay period. Data points indicate mean ± SEM.

alongside relative decreases to the expression of GluN2C and GluN2D subunits [21]. Moreover, as a brain region that continually exhibits some degree of neurogenesis, the DG is populated by both newly created and more mature granule cells [53] that can possess NMDArs with different combinations of subunits [54]. A second level of complexity comes from the fact that synaptic plasticity in the DG also exhibits age dependent changes [55, 56]. Not only is the DG populated by functional granule cells of various ages [53], the NMDAr composition of these cells can also play a role in the amount and type of plasticity they exhibit [54, 57]. Indeed, these experiments were initiated because we believed the controversy over the effects of EtOH on LTD in the DG [8, 9] might be due to differences in the ages of the animals used in the two studies. However, while LTD was once thought to be primarily an NMDAr mediated form of plasticity [58–61], it has become apparent that there are many studies where NMDAr antagonists do not completely block LTD expression in the DG [57, 62–64]. Currently the data indicates that the induction and expression of LTD in the DG can also involve mGluRs, voltage-gated Ca2+channels, and endocannabinoid receptors [12, 59, 62, 65–71]. Interestingly, we have also recently shown that acute EtOH exposure during adolescence can impact both endocannabinoid expression, and endocannabinoid receptor-dependent LTD [69, 71–73].

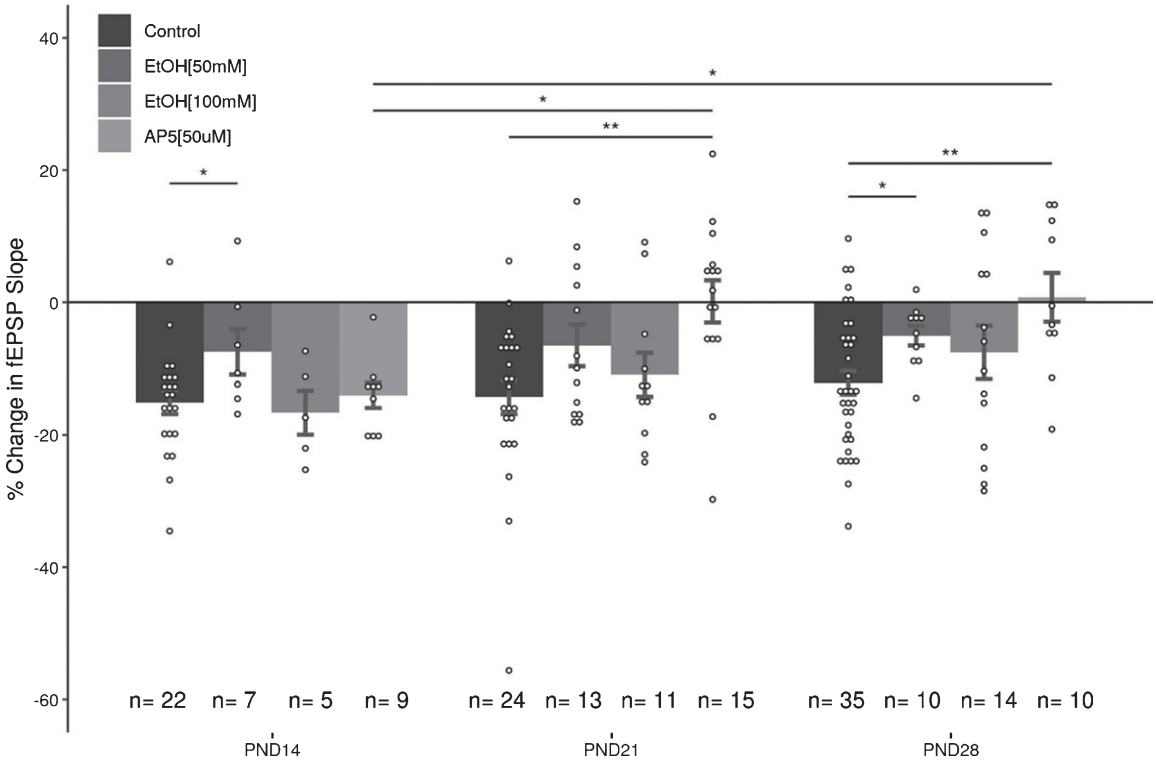

Fig. 7. Summary of effects of AP5 and EtOH (50&100 mM) on LTD in the juvenile DG. These data help illustrate that (1) the role of NMDArs in the induction and expression of LTD in the DG change during the juvenile period, and (2) that low (50 mM), but not high (100 mM), concentrations of EtOH can inhibit LTD expression during the juvenile period. Data points indicate mean ± SEM. $^{*}p < 0.05$; $^{**}p < 0.01$.

A particularly interesting methodological component of the current work was the presence of the redox agents Na-pyruvate and ascorbic acid in the perfusate used for the whole-cell experiments. These compounds were included in an attempt to reduce the effects of oxidative stress on the cells during the tissue preparation process, and throughout the experimental procedure, as NMDArs are sensitive to changes in oxidation and reduction [74–76]. NMDAr conductance is greater when the protein is in a reduced state, and oxidation of the receptor decreases the ionic conductance. Whether EtOH affects NMDArs differently depending on either the redox state of the local environment, or of the receptor itself, is currently unclear. In the future, this could be addressed using whole-cell patch clamp to determine if the sensitivity of NMDAr-EPSCs to EtOH changes with respect to the NMDAr redox state, which could be controlled with redox agents DTT and DTNB [75, 77].

In summary, the current data provide further support EtOH acting as a partial antagonist for NMDArs, and show that the impact of EtOH on LTD can be both dose and age-dependent during the juvenile period.

ACKNOWLEDGMENTS

The authors thank past Christie laboratory trainees T. Kannangara, B. Eadie, A. Titterness, R. Petersen, and F. Boehme for their input in the conception of these studies.

FUNDING

This work was funded by an NSERC Discovery grant and a CIHR project grant to BRC.

CONFLICT OF INTEREST

The authors have no conflict to report.

REFERENCES

[1] Organization WH. Global status report on alcohol and health 2018: executive summary. World Health Organization; 2018.

[2] Cservenka A, Brumback T. The Burden of Binge and Heavy Drinking on the Brain: Effects on Adolescent and Young Adult Neural Structure and Function. Frontiers in Psy-

chology. 2017;8:1111. https://doi.org/10.3389/fpsyg.2017.01111.

[3] Garcia-Moreno LM, Cimadevilla JM. Acute and chronic ethanol intake: effects on spatial and non-spatial memory in rats. Alcohol (Fayetteville, NY). 2012;46:757–62. https://doi.org/10.1016/j.alcohol.2012.08.001.

[4] White A, Hingson R. The burden of alcohol use: excessive alcohol consumption and related consequences among college students. Alcohol Research: Current Reviews. 2013;35:201–18.

[5] Olsen RW. GABAA receptor: Positive and negative allosteric modulators. Neuropharmacology. 2018;136:10–22. https://doi.org/10.1016/j.neuropharm.2018.01.036.

[6] Lima-Landman MTR, Albuquerque EX. Ethanol potentiates and blocks NMDA-activated single-channel currents in rat hippocampal pyramidal cells. FEBS Letters. 1989;247:61–7. https://doi.org/10.1016/0014-5793(89)81241-4.

[7] Lovinger DM, White G, Weight FF. Ethanol Inhibits NMDA-Activated Ion Current in Hippocampal Neurons. 1989;243:1721–4.

[8] Hendricson AW, Miao CLA, Lippmann MJ, Morrisett R a. Ifenprodil and ethanol enhance NMDAr-dependent long-term depression. The Journal of Pharmacology and Experimental Therapeutics. 2002;301:938–44. https://doi.org/10.1124/jpet.301.3.938.

[9] Izumi Y, Nagashima K, Murayama K, Zorumski CF. Acute effects of ethanol on hippocampal long-term potentiation and long-term depression are mediated by different mechanisms. Neuroscience. 2005;136:509–17. https://doi.org/10.1016/j.neuroscience.2005.08.002.

[10] Chandrasekar R. Alcohol and NMDA receptor: current research and future direction. Frontiers in Molecular Neuroscience. 2013;6:14. https://doi.org/10.3389/fnmol.2013.00014.

[11] Zorumski CF, Mennerick S, Izumi Y. Acute and chronic effects of ethanol on learning-related synaptic plasticity. Alcohol (Fayetteville, NY). 2014;48:1–17. https://doi.org/10.1016/j.alcohol.2013.09.045.

[12] Lovinger DM, Abrahao KP. Synaptic plasticity mechanisms common to learning and alcohol use disorder. Learning and Memory. 2018;25:425–34. https://doi.org/10.1101/lm.046722.117.

[13] Cull-Candy S, Brickley S, Farrant M. NMDA receptor subunits: diversity, development and disease. Current Opinion in Neurobiology. 2001;11:327–35. https://doi.org/10.1016/S0959-4388(00)00215-4.

[14] Cull-Candy SG, Leszkiewicz DN. Role of Distinct NMDA Receptor Subtypes at Central Synapses. Science's STKE. 2004;2004:re16 LP–re16. https://doi.org/10.1126/stke.2552004re16.

[15] Swartzwelder HS, Farr KL, Wilson WA, Savage DD. Prenatal exposure to ethanol decreases physiological plasticity in the hippocampus of the adult rat. Alcohol (Fayetteville, NY). 1988;5:121–4. https://doi.org/10.1016/0741-8329(88)90008-0.

[16] Li S-T, Kato K, Tomizawa K, Matsushita M, Moriwaki A, Matsui H, et al. Calcineurin plays different roles in group II metabotropic glutamate receptor- and NMDA receptor-dependent long-term depression. The Journal of Neuroscience: The Official Journal of the Society for Neuroscience. 2002;22:5034–41. https://doi.org/10.1523/JNEUROSCI.22-12-05034.2002.

[17] Mirshahi T, Woodward JJ. Ethanol sensitivity of heteromeric NMDA receptors: Effects of subunit assembly, glycine and NMDAR1 Mg2+-insensitive mutants. Neuropharmacology. 1995;34:347–55. https://doi.org/10.1016/0028-3908(94)00155-L.

[18] Blevins T, Mirshahi T, Chandler LJ, Woodward JJ. Effects of Acute and Chronic Ethanol Exposure on Heteromeric N-Methyl-d-Aspartate Receptors Expressed in HEK 293 Cells. Journal of Neurochemistry. 2002;69:2345–54. https://doi.org/10.1046/j.1471-4159.1997.69062345.x.

[19] Wright JM, Peoples RW, Weight FF. Single-channel and whole-cell analysis of ethanol inhibition of NMDA-activated currents in cultured mouse cortical and hippocampal neurons. Brain Research. 1996;738:249–56. https://doi.org/10.1016/S0006-8993(96)00780-9.

[20] Ariwodola OJ, Crowder TL, Grant KA, Daunais JB, Friedman DP, Weiner JL. Ethanol Modulation of Excitatory and Inhibitory Synaptic Transmission in Rat and Monkey Dentate Granule Neurons. Alcoholism: Clinical & Experimental Research. 2003;27:1632–9.

[21] Mameli M. Developmentally Regulated Actions of Alcohol on Hippocampal Glutamatergic Transmission. Journal of Neuroscience. 2005;25:8027–36. https://doi.org/10.1523/JNEUROSCI.2434-05.2005.

[22] Xu M, Smothers CT, Trudell J, Woodward JJ. Ethanol inhibition of constitutively open N-methyl-D-aspartate receptors. The Journal of Pharmacology and Experimental Therapeutics. 2012;340:218–26. https://doi.org/10.1124/jpet.111.187179.

[23] Ren H, Zhao Y, Dwyer DS, Peoples RW. Interactions among positions in the third and fourth membrane-associated domains at the intersubunit interface of the N-Methyl-D-aspartate receptor forming sites of alcohol action. Journal of Biological Chemistry. 2012;287:27302–12. https://doi.org/10.1074/jbc.M111.338921.

[24] Ronald KM, Mirshahi T, Woodward JJ. Ethanol Inhibition of N-Methyl-D-aspartate Receptors Is Reduced by Site-directed Mutagenesis of a Transmembrane Domain Phenylalanine Residue. Journal of Biological Chemistry. 2001;276:44729–35. https://doi.org/10.1074/jbc.M102800200.

[25] Thetford Smothers C, Woodward JJ. Effects of Amino Acid Substitutions in Transmembrane Domains of the NR1 Subunit on the Ethanol Inhibition of Recombinant N-Methyl-d-aspartate Receptors. Alcoholism: Clinical and Experimental Research. 2006;30:523–30. https://doi.org/10.1111/j.1530-0277.2006.00058.x.

[26] Collingridge GL, Bliss TV. Memories of NMDA receptors and LTP. Trends in Neurosciences. 1995;18:54–6.

[27] Pinar C, Fontaine CJ, Triviño-Paredes J, Lottenberg CP, Gil-Mohapel J, Christie BR. Revisiting the flip side: Long-term depression of synaptic efficacy in the hippocampus. Neuroscience and Biobehavioral Reviews. 2017;80:394–413. https://doi.org/10.1016/j.neubiorev.2017.06.001.

[28] Petersen RP, Moradpour F, Eadie BD, Shin JD, Kannangara TS, Delaney KR, et al. Electrophysiological identification of medial and lateral perforant path inputs to the dentate gyrus. Neuroscience. 2013;252:154–68. https://doi.org/10.1016/j.neuroscience.2013.07.063.

[29] R Core Team. R: A Language and Environment for Statistical Computing; 2018.

[30] Wickham H. ggplot2: Elegant Graphics for Data Analysis. Springer-Verlag New York; 2016.

[31] Aphalo PJ. gginnards: Explore the Innards of 'ggplot2' Objects; 2018.

[32] Dowle M, Srinivasan A. data.table: Extension of 'data.frame'; 2019.

[33] Zhu H. kableExtra: Construct Complex Table with 'kable' and Pipe Syntax; 2019.
[34] Xie Y. knitr: A General-Purpose Package for Dynamic Report Generation in R; 2018.
[35] Bates D, Maechler M, Bolker B, Walker S. lme4: Linear Mixed-Effects Models using 'Eigen' and S4; 2019.
[36] Urbanek S. png: Read and write PNG images 2013.
[37] Allaire JJ, Xie Y, McPherson J, Luraschi J, Ushey K, Atkins A, et al. rmarkdown: Dynamic Documents for R; 2018.
[38] Wickham H, Danenberg P, Eugster M. roxygen2: In-Line Documentation for R; 2018.
[39] Wickham H. tidyverse: Easily Install and Load the 'Tidyverse'; 2017.
[40] Wickham H, Bryan J. usethis: Automate Package and Project Setup; 2018.
[41] Stephens J, Simonov K, Xie Y, Dong Z, Wickham H, Horner J, et al. yaml: Methods to Convert R Data to YAML and Back; 2018.
[42] Morrisett R, Swartzwelder H. Attenuation of hippocampal long-term potentiation by ethanol: a patch- clamp analysis of glutamatergic and GABAergic mechanisms. J Neurosci. 1993;13:2264–72.
[43] Lahnsteiner E, Hermann A. Acute action of ethanol on rat hippocampal CA1 neurons: effects on intracellular signaling. Neuroscience Letters. 1995;191:153–6. https://doi.org/10.1016/0304-3940(95)11579-L.
[44] Puglia MP, Valenzuela CF. Ethanol acutely inhibits ionotropic glutamate receptor-mediated responses and long-term potentiation in the developing CA1 hippocampus. Alcoholism, Clinical and Experimental Research. 2010;34:594–606. https://doi.org/10.1111/j.1530-0277.2009.01128.x.
[45] Zhao Y, Ren H, Dwyer DS, Peoples RW. Different sites of alcohol action in the NMDA receptor GluN2A and GluN2B subunits. Neuropharmacology. 2015;97:240–50. https://doi.org/10.1016/j.neuropharm.2015.05.018.
[46] Hicklin TR, Wu PH, Radcliffe RA, Freund RK, Goebel-Goody SM, Correa PR, et al. Alcohol inhibition of the NMDA receptor function, long-term potentiation, and fear learning requires striatal-enriched protein tyrosine phosphatase. Proceedings of the National Academy of Sciences of the United States of America. 2011;108:6650–5. https://doi.org/10.1073/pnas.1017856108.
[47] Wu PH, Coultrap SJ, Browning MD, Proctor WR. Functional Adaptation of the N-Methyl- D -aspartate Receptor to Inhibition by Ethanol Is Modulated by Striatal-Enriched Protein Tyrosine Phosphatase and p38 Mitogen-Activated Protein Kinase. Molecular Pharmacology. 2011;80:529–37. https://doi.org/10.1124/mol.110.068643. NMDAR.
[48] Hughes BA, Smothers CT, Woodward JJ. Dephosphorylation of GluN2B C-terminal tyrosine residues does not contribute to acute ethanol inhibition of recombinant NMDA receptors. Alcohol. 2013;47:181–6. https://doi.org/10.1016/j.alcohol.2012.12.015.
[49] Fleming RL, Wilson WA, Swartzwelder HS. Magnitude and ethanol sensitivity of tonic GABAA receptor-mediated inhibition in dentate gyrus changes from adolescence to adulthood. Journal of Neurophysiology. 2007;97:3806–11. https://doi.org/10.1152/jn.00101.2007.
[50] Fricke RA, Prince DA. Electrophysiology of dentate gyrus granule cells. Journal of Neurophysiology. 1984;51:195–209. https://doi.org/10.1152/jn.1984.51.2.195.
[51] Ye GL, Song Liu X, Pasternak JF, Trommer BL. Maturation of glutamatergic neurotransmission in dentate gyrus granule cells. Developmental Brain Research. 2000;124:33–42. https://doi.org/10.1016/S0165-3806(00)00103-6.
[52] Pedroni A, Minh DD, Mallamaci A, Cherubini E. Electrophysiological characterization of granule cells in the dentate gyrus immediately after birth. Frontiers in Cellular Neuroscience. 2014;8:1–9. https://doi.org/10.3389/fncel.2014.00044.
[53] Praag H van, Schinder AF, Christie BR, Toni N, Palmer TD, Gage FH. Functional neurogenesis in the adult hippocampus. Nature. 2002;415:1030–4. https://doi.org/10.1038/4151030a.
[54] Ge S, Yang C-H, Hsu K-S, Ming G-L, Song H. A Critical Period for Enhanced Synaptic Plasticity in Newly Generated Neurons of the Adult Brain. Neuron. 2007;54:559–66. https://doi.org/10.1016/j.neuron.2007.05.002.
[55] Norris CM, Halpain S, Foster TC. Reversal of age-related alterations in synaptic plasticity by blockade of L-type Ca2+ channels. The Journal of Neuroscience: The Official Journal of the Society for Neuroscience. 1998;18:3171–9.
[56] Foster TC, Norris CM. Age-associated changes in Ca(2+)-dependent processes: relation to hippocampal synaptic plasticity. Hippocampus. 1997;7:602–12. https://doi.org/10.1002/(SICI)1098-1063(1997)7:6<602::AID-HIPO3>3.0.CO;2-G.
[57] Vasuta C, Caunt C, James R, Samadi S, Schibuk E, Kannangara T, et al. Effects of exercise on NMDA receptor subunit contributions to bidirectional synaptic plasticity in the mouse dentate gyrus. Hippocampus. 2007;17:1201–8.
[58] Christie BR, Abraham WC. NMDA-dependent heterosynaptic long-term depression in the dentate gyrus of anaesthetized rats. Synapse. 1992;10:1–6. https://doi.org/doi:10.1002/syn.890100102.
[59] Christie BR, Abraham WC. Priming of associative long-term depression in the dentate gyrus by θ frequency synaptic activity. Neuron. 1992;9:79–84. https://doi.org/10.1016/0896-6273(92)90222-Y.
[60] Dudek SM, Bear MF. Bidirectional long-term modification of synaptic effectiveness in the adult and immature hippocampus. The Journal of Neuroscience: The Official Journal of the Society for Neuroscience. 1993;13:2910–8.
[61] Mulkey RM, Malenka RC. Mechanisms underlying induction of homosynaptic long-term depression in area CA1 of the hippocampus. Neuron. 1992;9:967–75. https://doi.org/10.1016/0896-6273(92)90248-C.
[62] Trommer BL, Liu YB, Pasternak JF. Long-term depression at the medial perforant path-granule cell synapse in developing rat dentate gyrus. Developmental Brain Research. 1996;96:97–108. https://doi.org/10.1016/0165-3806(96)00104-6.
[63] Wang Y, Rowan MJ, Anwyl R. Induction of LTD in the dentate gyrus *in vitro* is NMDA receptor independent, but dependent on Ca2+ influx via low-voltage-activated Ca2+ channels and release of Ca2+ from intracellular stores. Journal of Neurophysiology. 1997;77:812–25.
[64] Camodeca N, Breakwell NA, Rowan MJ, Anwyl R. Induction of LTD by activation of group I mGluR in the dentate gyrus *in vitro*. Neuropharmacology. 1999;38:1597–606. https://doi.org/10.1016/S0028-3908(99)00093-3.
[65] O'Mara SM, Rowan MJ, Anwyl R. Metabotropic glutamate receptor-induced homosynaptic long-term depression and depotentiation in the dentate gyrus of the rat hippocampus *in vitro*. Neuropharmacology. 1995;34:983–9. https://doi.org/10.1016/0028-3908(95)00062-B.
[66] Chávez AE, Chiu CQ, Castillo PE. TRPV1 activation by endogenous anandamide triggers postsynaptic long-

term depression in dentate gyrus. Nature Neuroscience. 2010;13:1511–8. https://doi.org/10.1038/nn.2684.

[67] Han J, Kesner P, Metna-Laurent M, Duan T, Xu L, Georges F, et al. Acute cannabinoids impair working memory through astroglial CB1receptor modulation of hippocampal LTD. Cell. 2012;148:1039–50. https://doi.org/10.1016/j.cell.2012.01.037.

[68] Christie BR, Schexnayder LK, Johnston D. Contribution of voltage-gated Ca2+ channels to homosynaptic long-term depression in the CA1 region *in vitro*. Journal of Neurophysiology. 1997;77:1651–5. https://doi.org/10.1152/jn.1997.77.3.1651.

[69] Peñasco S, Rico-Barrio I, Puente N, Gómez-Urquijo SM, Fontaine CJ, Egaña-Huguet J, et al. Endocannabinoid long-term depression revealed at medial perforant path excitatory synapses in the dentate gyrus. Neuropharmacology. 2019;153:32–40. https://doi.org/10.1016/j.neuropharm.2019.04.020.

[70] Penasco S, Rico-Barrio I, Puente N, Fontaine CJ, Ramos A, Reguero L, et al. Intermittent ethanol exposure during adolescence impairs cannabinoid type 1 receptor-dependent long-term depression and recognition memory in adult mice. Neuropsychopharmacology: Official Publication of the American College of Neuropsychopharmacology. 2020;45:309–18. https://doi.org/10.1038/s41386-019-0530-5.

[71] Bonilla-Del Riotao I, Puente N, Penasco S, Rico I, Gutierrez-Rodriotaguez A, Elezgarai I, et al. Adolescent ethanol intake alters cannabinoid type-1 receptor localization in astrocytes of the adult mouse hippocampus. Addiction Biology. 2019;24:182–92. https://doi.org/10.1111/adb.12585.

[72] Choi Y, Chen HV, Lipton SA. Three pairs of cysteine residues mediate both redox and zn2+ modulation of the nmda receptor. The Journal of Neuroscience: The Official Journal of the Society for Neuroscience. 2001;21:392–400. https://doi.org/21/2/392 [pii].

[73] Bodhinathan K, Kumar A, Foster TC. Intracellular Redox State Alters NMDA Receptor Response during Aging through Ca2+/Calmodulin-Dependent Protein Kinase II. Journal of Neuroscience. 2010;30:1914–24. https://doi.org/10.1523/JNEUROSCI.5485-09.2010.

[74] Talukder I, Kazi R, Wollmuth LP. GluN1-specific redox effects on the kinetic mechanism of NMDA receptor activation. Biophysical Journal. 2011;101:2389–98. https://doi.org/10.1016/j.bpj.2011.10.015.

[75] Lipton SA, Rayudu PV, Choi YB, Sucher NJ, Chen HS. Redox modulation of the NMDA receptor by NO-related species. Progress in Brain Research. 1998;118:73–82. https://doi.org/10.1007/PL00000638.